

## Article

# Identification Efficiency in Dynamic UHF RFID Anticollision Systems with Textile Electronic Tags

Bartosz Pawłowicz <sup>1,\*</sup> , Kazimierz Kamuda <sup>1</sup> , Mariusz Skoczylas <sup>1</sup>, Piotr Jankowski-Mihułowicz <sup>1</sup> ,  
Mariusz Węglarski <sup>1,\*</sup>  and Grzegorz Laskowski <sup>2</sup>

<sup>1</sup> Department of Electronic and Telecommunications Systems, Rzeszów University of Technology, ul. Wincentego Pola 2, 35-959 Rzeszów, Poland

<sup>2</sup> Research & Development Center of Esotiq & Henderson S.A., ul. Budowlanych 31c, 80-298 Gdańsk, Poland

\* Correspondence: barpaw@prz.edu.pl (B.P.); wmar@prz.edu.pl (M.W.); Tel.: +48-1785-44708 (B.P. & M.W.)

**Abstract:** The study on the numerical model of communication processes implemented in RFID systems, in which textile electronic (RFIDtex) tags are used, is presented in the paper. The efficiency analysis covers the case of dynamic identification of a large amount of RFIDtex tags that are located in a spatial interrogation zone of a typical Internet of Textile Things (IoTT) application. Simulations carried out in order to verify the efficiency of the identification process are confirmed by measurements on the dedicated laboratory stand. Since the application of the experiment is located in the area of a maintenance-free store to detect and distinguish textile products, particular attention is paid to reconstruction of conditions and object arrangements that are typical for this type of space. The model and experiment are developed on the basis of RFIDtex transponders that are restricted under the patent claim PL231291. The obtained results prove that within the scope of the assumed number of RFIDtex transponders, the user has great freedom in choosing the parameters of the communication protocol.

**Keywords:** RFIDtex systems; textronic transponder; identification efficiency; dynamic RFID systems; anticollision protocol



**Citation:** Pawłowicz, B.; Kamuda, K.; Skoczylas, M.; Jankowski-Mihułowicz, P.; Węglarski, M.; Laskowski, G. Identification Efficiency in Dynamic UHF RFID Anticollision Systems with Textile Electronic Tags. *Energies* **2023**, *16*, 2626. <https://doi.org/10.3390/en16062626>

Academic Editor: Corrado Florian

Received: 21 January 2023

Revised: 6 March 2023

Accepted: 8 March 2023

Published: 10 March 2023



**Copyright:** © 2023 by the authors. Licensee MDPI, Basel, Switzerland. This article is an open access article distributed under the terms and conditions of the Creative Commons Attribution (CC BY) license (<https://creativecommons.org/licenses/by/4.0/>).

## 1. Introduction

### 1.1. State-of-the-Art

The presented study contains the characteristics of the communication model prepared for the radio frequency identification (RFID) system [1,2]. The concept and methodology of efficiency analysis cover the definition of the radio interface for the proposed functional assumptions of logistics systems used in the textile industry. The research is focused on the development of Internet of textile things (IoTT), in which textile electronic RFID transponders, also known in technical language as textronic RFID (RFIDtex) tags, are used to mark fabric products.

The subject of RFID technology implemented for identification of textile products has been widely reflected in presented and published contemporary studies for several years. Concepts and assumptions of similar smart textiles have been extensively described in some works [3–5]. Various constructions of transponders dedicated to applications in broadly understood textronics are analysed in works [6–10], and the benefits and limitations of tags in standard and textronic versions are analysed in the study [11]. The presented research set-up is based on technical capabilities of commercially available: (1) RFID devices, such as RFID tag chips, read/write devices (RWD), and RWD antennas; (2) standardized communication protocols and relevant standards regulating the operation and parameters of radio devices; (3) methods of parameter verification in RFID systems.

According to the operation principles of the RFID systems, the electronic tags are identified in the interrogation zone (IZ). The issue of the interrogation zone is well known

and presented in the literature [1,2]. In the IZ, the field, energy, and communication conditions have to be met in order to perform contactless identification (Figure 1).

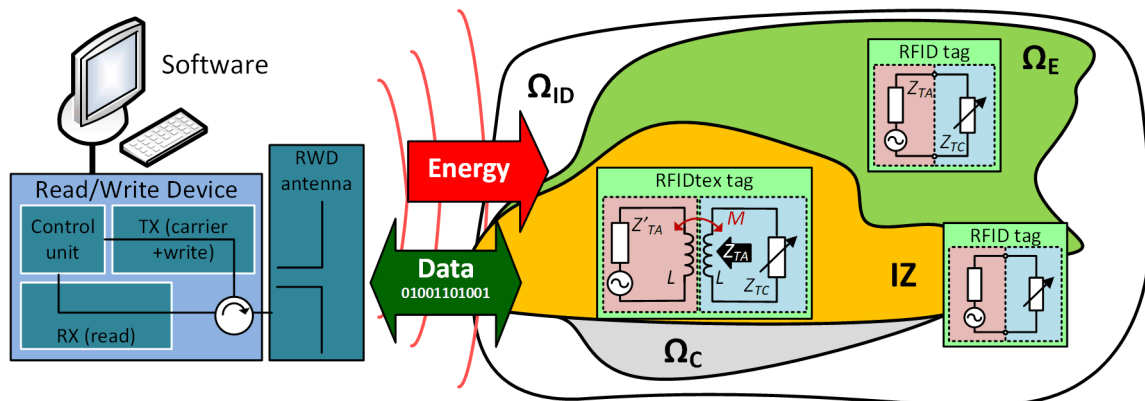


**Figure 1.** The principle of RFID system operation: RFID tag—passive transponder made in standard RFID technology; RFIDtex tag—textronic RFID transponder made according to PL231291 patent idea;  $\Omega_{ID}$ —application space of RFID system implementation;  $\Omega_E$ —zone where field and energy conditions are met;  $\Omega_C$ —zone where communication condition may be met; IZ—interrogation zone where field, energy, and communication conditions are met together;  $Z_{TA}$ —antenna impedance;  $Z'_{TA}$ —antenna impedance without coupling system;  $Z_{TC}$ —chip impedance;  $M$ —coupling inductance;  $L$ —inductance of coupling circuits; TX—transmitter; RX—receiver.

In the case of static RFID systems, the presence of transponders in the interrogation zone means that all of them can be read/identified after a certain time [1,2]. In this respect, the identification efficiency, understood as the ratio of the number of read tags to the number of tags subjected to the interrogation, is equal to one (100%). Since the time is not limited, the interrogation zone is restricted to field and energy conditions of the electromagnetic environment that have to be met in order to perform the recognition process. The energy conditions are understood as the minimum power delivered to the tags in order to power them. The field conditions are related to the value of the electromagnetic field strength necessary to induce the minimum voltage at the tag antenna terminals.

In the case of dynamic RFID systems, in which the time of identification is limited, the analytical model, that is based only on the limited interrogation zone, becomes insufficient. In the basic literature, it can be found that the identification efficiency (required or obtained), which can be less than 1, has to be taken into consideration in this case. The anticollision mechanism that is used in the dynamic systems is particularly sensitive to communication conditions [12]. The communication conditions are a set of standard protocol parameters responsible for the time of data exchange between the transponders and the RWD. The data transmission speed and hence time and efficiency of the identification are determined by the methods of multiple access to the radio channel, the structure of transmitted data packets, time parameters of the protocol, data collisions, interruptions in data transmission, etc.

In the work [13], authors propose a method in which a dynamic regulation of the protocol frame length is used. The method allows investigators to adjust the time of reading tags, and thus to increase the efficiency of the identification process. An advanced regulation of the slot number in the DFSA (Dynamic Framed Slotted Aloha) multi-access protocol used in the RFID technology is proposed in a publication [14], and a slightly modified approach is described in [15]. In studies [16,17], the authors analyze predictive mechanisms for adjusting the frame length of inventory rounds. They use the Aloha-based algorithm in which the prediction is based on the knowledge about the behavior and results of previously performed inventory rounds. In papers [18,19], the authors try to use mathematical methods to estimate protocol parameters in order to find the most effective identification of a given transponder population. The method of selecting gaps in the DFSA

frame is considered in the research [20]. Instead of calculating the number of types of gaps, the authors propose a method based on the duration of each gap. They introduce an algorithm that takes into account the weights of frame components on the efficiency of the simulated process. In the work [21], the proposed algorithm is aimed to increase the RFID system efficiency by an innovative method of detecting lost tags. The so-called "lost" tag results from errors in the reading and identification process. In [22], it is proposed to divide the IZ into sub-zones analyzed by the sequential method.

Basing on the aforementioned studies and their own experiences (e.g., [23]), the authors of presented research propose a new algorithm for dividing the interrogation zone. They consider both the spatial and time aspects of the system operation. The simulation of a dynamic system is obtained by using cyclically repeated inventory rounds. The method of estimating the number of transponders not recognized in an inventory round is also implemented in the algorithm. In addition, it is referred to the spatial sections of the interrogation zones and subsequent inventory rounds.

### 1.2. Research Idea

In the developed communication model, the authors consider the RFID system operating in the UHF band (860–960 MHz), with particular emphasis on the parameters and the frequency band of 865.6–867.6 MHz, defined in the ETSI EN 302 208 standard and compliant with the requirements of the electronic product code, standardized in ISO/IEC 18000-63/EPC Class 1 Gen 2 for the European market [24]. In order to avoid the unfavorable environmental impact (e.g., instability of electromagnetic field or effects related to multipath propagation and interference) and fully meet the requirements of the standards, the measurements were carried out in a shielded semi-anechoic chamber [25].

The numerical model and experiment are developed on the basis of textronic RFIDtex transponders that are restricted under the authors' patent claim PL231291 (Figure 2a). The SL3S1214 UCODE 7m chips from NXP Semiconductor (Eindhoven, Netherlands) [26] (read sensitivity:  $-21$  dBm, write sensitivity:  $-16$  dBm, compatible with EPC Class 1 Gen 2 [27]) are used in the work. In the EPC Class 1 Gen 2 communication protocol, the RWD communicates with the transponders by modulating the carrier frequency using DSB-ASK (Double Side Band-Amplitude Shift Keying), SSB-ASK (Single Side Band-ASK) or PR-ASK (Phase Reversal-ASK) with PIE (Pulse Interval Encoding) coding. The tags responding to the commands of the RWD use the modulation of the reflected wave with FM0 or Miller transmission coding. In order to read multiple tags, the RFID system has to use a multiple access technique. In the case of systems based on the EPC Class 1 Gen 2 standard, the multiple access protocol is based on the DFSA method.

Typical RFID tags consist of two main parts, the antenna and the chip (RFID tag in Figure 1). The most important thing when developing a new transponder is to design the antenna circuit in such a way that its impedance, including the matching circuit, is coupled to the input impedance of the RF front-end in the microelectronic circuit (RFID chip). In the case of standard constructions, in which chips are galvanically connected to antenna terminals (e.g., by gluing or soldering), the design process is well known, and many times described in the literature. In the case of the RFIDtex tag (Figure 2a), the antenna module and the microelectronic module are placed on separate substrates. Both parts of the system are connected by the coupling circuit. The issues of designing such a device have been described in [28] in terms of meeting the field and electrical conditions. So far, the authors have not considered the terms of communications in any publication. Thus, this article complements the RFIDtex tag synthesis process in this aspect.

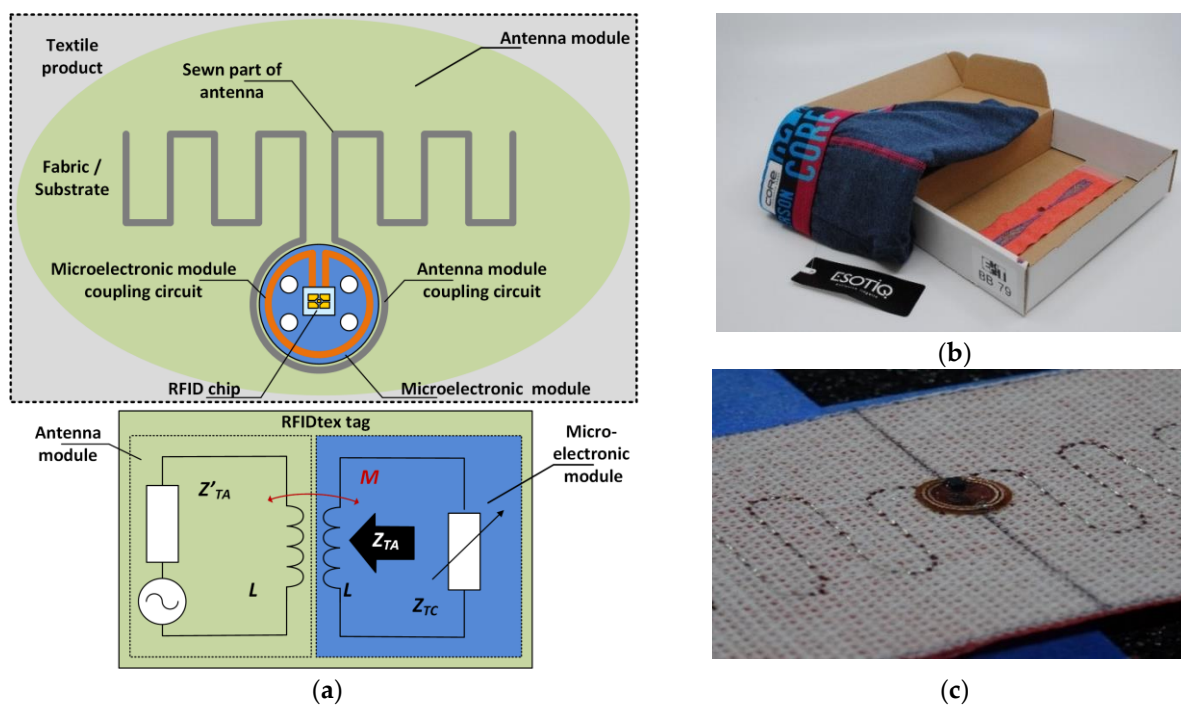


**Figure 2.** Textile RFID transponder (RFIDtex tag): (a) idea of transponder construction; (b) example of embroidered antenna module in under laboratory tests of target application; (c) microelectronic module of RFIDtex transponder with connected to sewn antenna in meander shape.

It is also necessary to highlight the general sense of considered problems related to the synthesis of the RFIDtex transponders. First of all, their use allows avoiding problems with the assembly of the RFID chip on a flexible and uneven textile substrate, and thus avoid many problems related to the protection of the electronic system against the environmental impact [28,29]. The antenna module (antenna radiator together with the matching and coupling circuit) can be made by any technique known from the clothing industry using conductive threads (Figure 2b,c). In turn, the microelectronic module can be made in an electronics company as a typical electronic device (e.g., in the form of a tablet, button, bead) and as a semi-finished product it can be attached to a textile product by sewing methods (Figure 2c). It is also important to have the possibility to use the RFIDtex transponders at all stages of the life cycle of a textile product, i.e., in the stages of production, quality control, broadly understood distribution and use, and finally utilization [30–32].

The essence of the conducted and presented research is to confirm the usable features of the textronic RFID transponders developed as part of previous works [28,30] and description of the PL231291 patent. The innovative idea of the RFIDtex tag is to manufacture its antenna in the form of an application (by sewing or embroidering) with a conductive thread and coupling its electronic chip with the antenna radiator without a galvanic interconnection. In order to justify the usefulness of the device in typical implementations in the textile world, the interrogation zone, the main parameter of any RFID system, has to be considered. So far, in previous publications [28,30], only field and electrical conditions were analysed, while only communication properties were mentioned. In presented work, the RFIDtex transponders are subjected to simulations and measurements on the experimental stand in the course of the multiple identification process, taking into account the parameters and factors shaping both telecommunications as well as field and energy conditions.

In order to prove the elaborated conception, the numerical model of communication in the dynamic anticollision RFID system is developed and presented in Section 2.1. Next, in Section 2.2 the setup of laboratory IoT application is discussed. Section 3 is devoted to a detailed explanation of the obtained results. The dependence of the efficiency vs. the number of objects in the interrogation zone is considered on the numerical model

for various parameters that can be set in the communication channel (Section 3.1). The simulation outcomes are confirmed by measurements performed in quasi-real application of IoTT environment (Section 3.2). The paper is concluded in Section 4.

## 2. Assumptions for Synthesis

### 2.1. Numerical Model

In dynamic RFID systems, objects with transponders are identified in a specified finite time determined by inventory rounds. The process is based on the RWD’s queries and tags’ responses sent in accordance with the established communication protocol. Therefore, it was assumed that all objects move by a certain distance  $\Delta d$  during one inventory round. The rounds form sections of the interrogation zone, and results from the required identification time, the assumed size of IZ and the duration of one inventory round (Figure 3a):

$$\Delta d = \frac{d_{IZ}}{T_i} \times T_r, \tag{1}$$

where:  $T_i$ —identification time,  $d_{IZ}$ —dimension of IZ,  $T_r$ —duration of inventory round,  $\Delta d$ —section of IZ that is determined by moving transponders in one inventory round. The sections are stationary—they do not move with transponders.

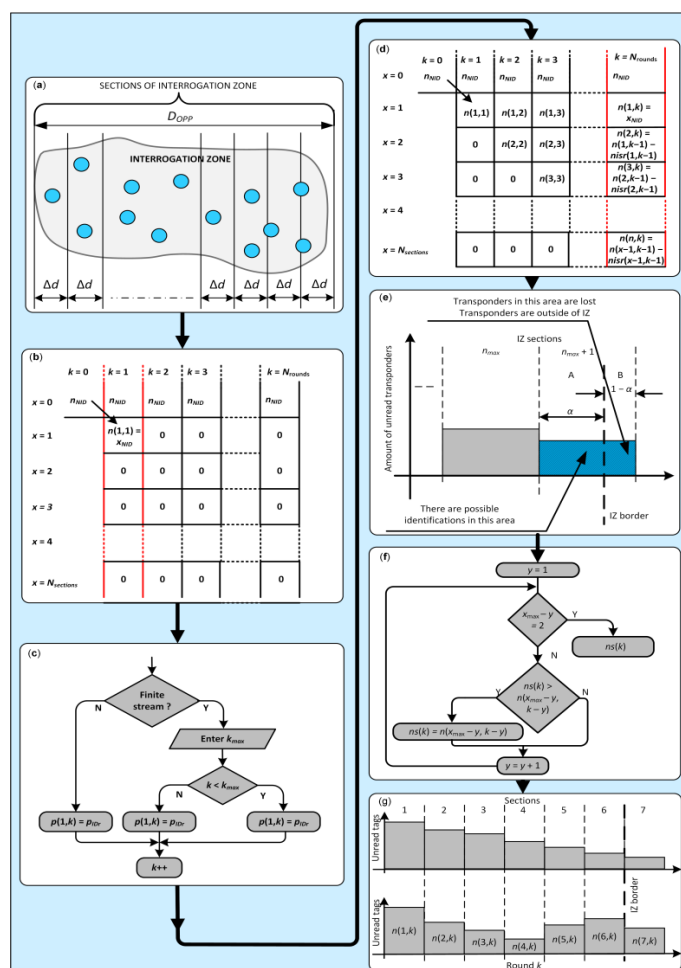


**Figure 3.** Dynamic system model: (a) division into sections in IZ; (b) matrix describing RFID system state in the first round of identification; (c) algorithm for introducing new transponders to the first section of IZ in subsequent rounds; (d) system state in  $k$ -th round; (e) estimating lost tags; (f) estimation algorithm of lost tags; (g) system state at infinite persistence time and at finite persistence time in selected round  $k$ .

The first section of the interrogation zone is designated as  $n_1$  and new transponders appear in it during the identification process. The last section is described by  $n_{max}$ :

$$n_{max} = n \left( \frac{d_{IZ}}{\Delta d} \right)_{max}. \quad (2)$$

For convenience, the concept of the system state is introduced into further considerations. The system state is the number of unread transponders that are in the IZ. It is a function of time and may vary from round to round. The system state consists of the number of tags unread in individual sections. Thus, the section state can be determined for subsequent rounds.

During the identification process carried out in a single round, the RWD's queries are answered by transponders located in the entire IZ. As a consequence, the system state has to be described in the spatial and time domain and following requirements have to be involved in the numerical model:

1. Transponders in the IZ are subjected to identification in a given inventory round;
2. The probability of tag recognition does not depend on its location in the IZ;
3. The number of unread transponders in a moving group decreases over time as a result of performed identifications;
4. The number of transponders read in a round and section is proportional to the number of previously unread tags in that section.

The system state varies between sections and rounds. In order to model the described problem, the approach proposed in [22] is developed and a matrix notation is used to represent the system state. It is generally assumed that the columns of matrix set correspond to the successive inventory rounds, whereas the rows to the successive sections (Figure 3b). The following matrices are defined to describe the system operation:

- **P** with terms  $p(n,k)$ , equals number of tags unread in section  $n$  and round  $k$ ;
- **PISR** with terms  $pisr(n,k)$ , equals number of correct identifications in section  $n$  and round  $k$ ;
- **PIR** with terms  $pir(k)$ , equals number of identifications in IZ in round  $k$ ;
- **PS** with terms  $ps(k)$ , equals number of tags lost in round  $k$ , tags that have not yet been read.

When analyzing the system state, it is important to relate the section state in a given round with the section state in the previous round. In the discussed method, this relationship can be described as follow:

$$p(n,k) = p(n-1,k-1) - pisr(n-1,k-1), \quad (3)$$

where  $p(0,0) = 0$  and  $pisr(0,0) = 0$ . The formula expresses the fact that the number of transponders that are not read in a given section at the beginning of a round is equal to their number in the previous section at the beginning of the previous round minus the number of transponders that occurred in the previous section and round.

As follows the made and justified assumptions, the total number of identifications that takes place in a round in the entire IZ is divided into individual sections in proportions depending on the size of these sections before identification. This number is expressed by the formula:

$$pisr(n,k) = pir(k) \frac{p(n,k)}{\sum_{i=1}^{n_{max}} p(i,k)}. \quad (4)$$

The number of correct identifications depends on the number of identifications in round  $k$  in the entire IZ ( $pir(k)$ ), and the ratio of the number of unread transponders in section  $n$  and round  $k$  and the number of unread transponders in the entire IZ at the beginning of this round (Figure 3d).

The number of transponders lost in the round  $k$  can be determined from the relationship:

$$ps(k) = p(n_{max} + 1, k) = p(n_{max}, k - 1) - p_{isr}(n_{max}, k - 1). \quad (5)$$

The proposed model covers various cases of dynamic RFID identification systems. Situations for finite or infinite groups of transponders passing through the IZ can be considered in the calculations. Moreover, since the stream of objects entering the IZ may have both regular or random distribution, the rate of their entry per second is assumed as one of the main parameters. The transponders enter the IZ at the number of  $p_{IDr}$  (transponders/round) and it is recorded in successive columns of the first row of the matrix  $\mathbf{P}$ ; the rows correspond to the sections of the IZ. The fragment of the algorithm is presented in Figure 3c. Further, a method for estimating lost tags in a round is implemented in order to determine whether all transponders in the IZ are read. It should be noticed that the boundary of IZ does not always coincide with the boundary of the last section into which the area is divided. The situation where the last section expressed by  $n_{max} + 1$  is only partially located in the IZ is shown in Figure 3e. The part A is in the IZ while the part B is outside it. The coefficient  $\alpha$  is introduced to determine what part of the last section is in the IZ. It is described by the relation:

$$\alpha = \frac{d_{OPZ} - \Delta d \times n_{max}}{\Delta d}. \quad (6)$$

Due to the fact that there may still be identifications in the part A of the section  $n_{max} + 1$ , although the tags in the part B are lost, it can be written that the total number of unread transponders is equal:

$$pc(k) = \sum_{i=1}^{n_{max}} p(i, k) + p(n_{max} + 1, k). \quad (7)$$

Since total number of identifications in a given inventory round  $k$  is equal  $p_{ir}(k)$ , the number of lost transponders  $ps(k)$  can be expressed by the formula:

$$ps(k) = p(n_{max} + 1, k) \times (1 - \alpha) + p(n_{max} + 1, k) \times \alpha - p_{ir}(k) \frac{p(n_{max} + 1, k) \times \alpha}{\sum_{i=1}^{n_{max}} p(i, k)}. \quad (8)$$

It means that the number of lost transponders in the round  $k$  is equal to the sum of unread transponders in the parts A and B of section  $n_{max} + 1$  minus the number of recognized transponders during a given round in the part A. It is presented in the form of algorithm in Figure 3f and is described as:

$$ps(k) = p(n_{max} + 1, k) \times \left[ 1 - \alpha \frac{p_{ir}(k)}{\sum_{i=1}^{n_{max}} p(i, k)} \right]. \quad (9)$$

Another aspect of the dynamic identification is the persistence time  $T_{per}$  of transponders. Under infinite persistence conditions, a tag is only read once—an exemplary distribution of unread transponders can be presented as in Figure 3g. But, in real life, every tag is read multiple times during the identification session and the time in which it holds the recognition flag is finite—after this time, the tag is read again. Thus, in the case of a finite persistence time, the observed system state changes as shown in Figure 3g. If the number of unread transponders in section  $n$  and round  $k$  is  $p(n, k)$ , then the number in the next section and round  $k$  cannot be greater:

$$p(n, k) \geq p(n + m, k + m), \quad m = 1, 2, 3, \dots, \quad n + m \leq n_{max} + 1, \quad (10)$$

$$ps(k) = p(n_{max} + 1, k) \leq p(n_{max} - m, k - m), \quad m = 0, 1, 2, 3, \dots, \quad n_{max} - m \geq 1, \quad (11)$$

The persistence time is not directly present in the loss estimation algorithm. However, it is present by the fact that for some rounds and sections inequality (10) is not satisfied.

The value of this time affects the parameter  $m$  for which this inequality is false, and further the right side of this inequality is the number of lost transponders in a given round.

Based on the presented dependencies, which are the basis of the proposed model, the block diagram of the algorithm for simulating the dynamic RFID system can be formulated as in Figure 4.

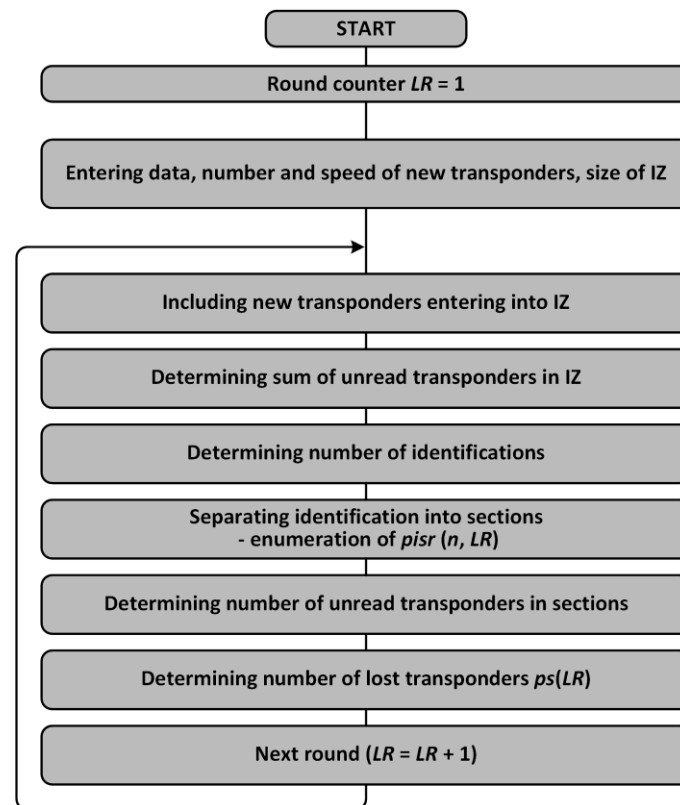


**Figure 4.** Dynamic system model—simplified simulation diagram of identification procedure.

Data from the transponders to the RWD are sent by means of modulation of the reflection coefficient of the backscattered carrier wave. The  $BLF$  subcarrier frequency is used, and it can be set in the range of 40 kHz–640 kHz. One period of this subcarrier is therefore in the range of 25  $\mu$ s–1.5625  $\mu$ s, and it is denoted as  $T_{pri}$ . The  $BLF$  frequency is related to the  $T_{Rcal}$  parameter in a way resulting from the relationship:

$$BLF = \frac{DR}{T_{Rcal}} \quad (12)$$

where the division ratio  $DR$  can take two values given in Table 1.

**Table 1.** DR parameter values in dependence on the  $BLF$  frequency.

<i>BLF</i> Frequency Range, kHz	<i>DR</i> Value
40–95	8
95–465	8 or 64/3
465–640	64/3

Free choice of the  $DR$  parameter in the frequency range 95 kHz–465 kHz allows for partially flexible selection of the  $T_{Rcal}$  time at a fixed  $BLF$  frequency or vice versa. The  $T_{pri}$

time is the basis for determining the duration of the  $T_{bTR}$  bits in the transponder-RWD transmission (this time is the same for bits 0 and 1) according to the dependence:

$$T_{bTR} = \frac{M}{BLF} = M \times T_{pri} \tag{13}$$

where for FM0 coding  $M = 1$ , and for Miller coding  $M = 2, 4$  or  $8$ . The  $M$  parameter determines how many  $BLF$  frequency periods fall on one bit of transmitted data. The most extensive response of the transponder to the Query reader command can be as shown in Figure 5.

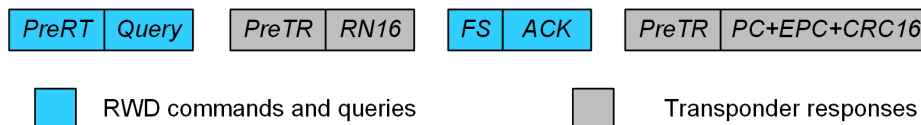


Figure 5. Sequence of RWD commands and transponder responses.

If the slot is the first slot in the inventory round, it is started with the *Query* command preceded by a preamble. The  $P_{reRT}$  preamble contains information defining the transmission speed between the RWD and the transponder, while the *Query* command contains, among others, information about the  $T_{Rext}$  parameter defining the length of the  $P_{reTR}$  preamble (Table 2) and may take the value 0 or 1. If a given slot is another slot in round, the transponder response is initiated by the *QueryRep* command.

Table 2.  $T_{PreTR}$  preamble lengths for different encoding types and different  $T_{Rext}$  values.

Encoding Type	$T_{PreTR}$	
	$T_{Rext} = 0$	$T_{Rext} = 1$
FM0	$6 \times T_{bTR}$	$18 \times T_{bTR}$
Miller	$10 \times T_{bTR}$	$22 \times T_{bTR}$

If a round needs to be modified due to empty slots or collisions, a slot can be started by the *QueryAdjust* command. Both of these commands are preceded by *FS* frame synchronization signals to maintain communication consistency. In response to one of the above three commands, the transponder replies with its *RN16* number preceded by a preamble. The *RN16* number is a unique 16-bit address of the transponder valid only during a single inventory round and generated at the time of receiving the *Query* command. In case of correct receipt of the transponder address by the RWD, the *ACK* confirmation of correct communication is followed, preceded by a frame synchronization signal, to which the transponder sends a preamble and then components of the electronic product code EPC. If the EPC code along with the PC auxiliary data and 16-bits CRC (Cyclic Redundancy Check) error detection code are correctly sent (128 bits in total), the reader issues one of the commands starting the next time slot. In the event of errors in the EPC code, the RWD sends the *NAK* command, which informs that the given transponder has not been correctly recognized and cannot change its status to read, which results in its further participation in the inventory round. Then the RWD starts another slot. The structure of a frame verified experimentally is presented in Figure 6.

According to the provisions of the standard, both FM0 and Miller coding end, the transponder transmission with End-of-Signaling symbol. Therefore, in reality these transmissions are longer (Table 3).

On the basis of the given dependencies and parameters, it is possible to determine the lengths of complete time slots that occur when reading transponders. Each of the slot types can start with one of the three RWD commands and it can be a slot with correct identification, an empty slot, a slot with data collision, or a slot with “started” identification and unfinished due to transmission errors. Data structure in these slots is shown in Figure 7.

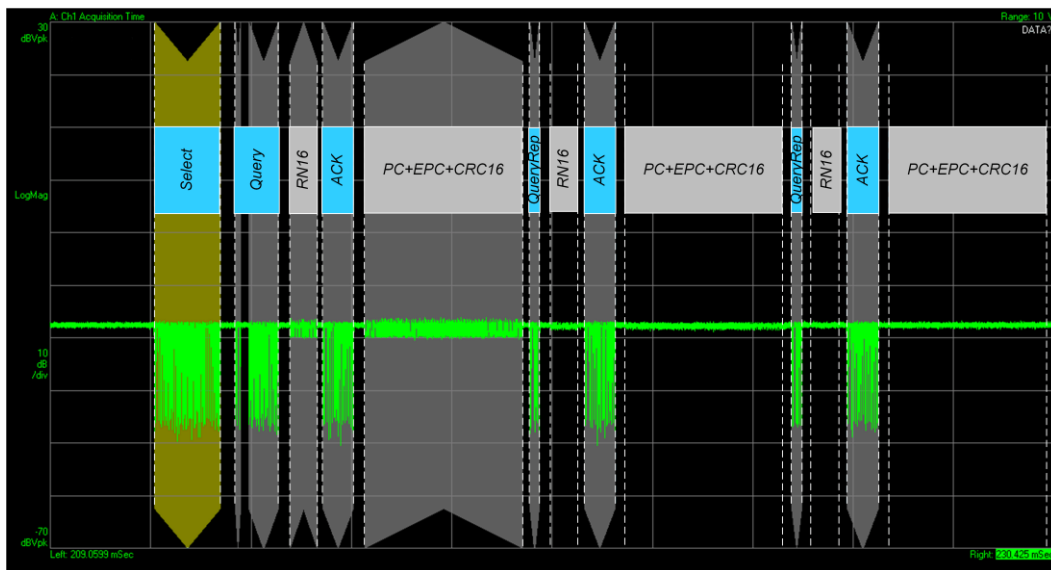


Figure 6. Structure of a single timeslot in the EPC protocol.

Table 3. The response times of the transponder expressed by the time  $T_{bTR}$ .

Transponder Response	Response Time
<i>RN16</i>	$(16 + 1) \times T_{pri}$
PC + EPC + CRC16	$(128 + 1) \times T_{pri}$

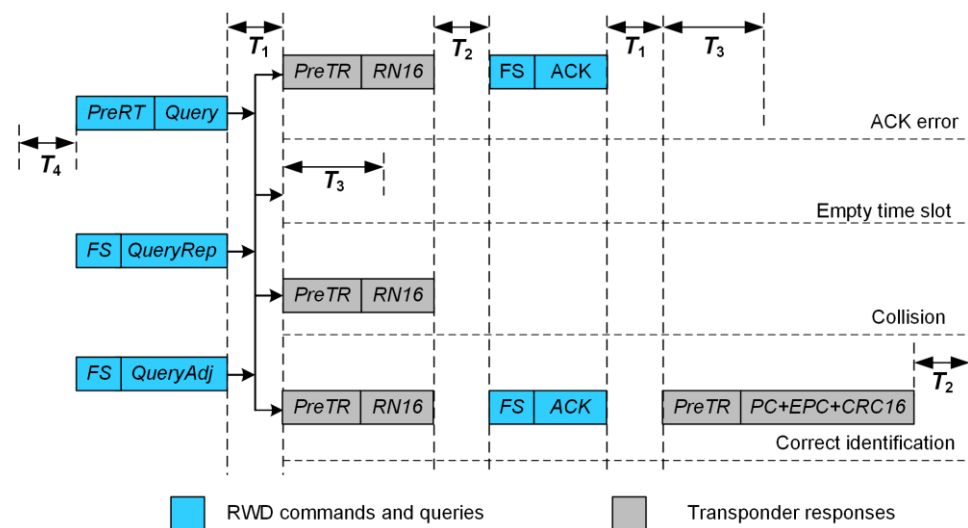


Figure 7. Presentation of the structure of time slots in the case of correct identification, data collision, empty slot, and incorrect confirmation of the *RN16* number.

The time intervals  $T_1$ – $T_4$  shown in this Figure 7 are the predicted delay time intervals between reader/programmer queries and transponder responses. The delay time  $T_4$  is the minimum time interval between successive rounds of the inventory. The time ranges  $T_1$ – $T_4$  are not strictly defined, the standard only provides ranges of values for them, and for the purposes of the developed model, the values listed in Table 4 are adopted.

**Table 4.** Summary of the length of pauses between RWD commands and transponder responses.

	Assumed Values	Requirements of the Standard
$T_1$	$T_{RTcal}$	$\max\{T_{RTcal}, 10 \times T_{pri}\} \pm 2 \mu s$
$T_2$	$10 \times T_{pri}$	$3 \times T_{pri} < T_2 < 20 \times T_{pri}$
$T_3$	$2 \times T_{pri}$	$> 0 \times T_{pri}$
$T_4$	$2 \times T_{RTcal}$	$2 \times RTcal$

Finally, the time of particular types of reader queries can be expressed using the dependencies listed in Table 5, while the sessions of the actual data exchange will have lengths described by the dependencies listed in Table 6.

**Table 5.** The duration of each type of query used by the RWD.

RWD Command	The Duration of the Command
<i>PreRT + Query</i>	$2 \times T_{RTcal} + 12.5 \mu s + T_{ari} + 2 \times pivot \times T_{ari} + T_{TRcal} + T_{que}$
<i>FS + QueryRepeat</i>	$12.5 \mu s + T_{ari} + 2 \times pivot \times T_{ari} + T_{qrep}$
<i>FS + QueryAdjust</i>	$12.5 \mu s + T_{ari} + 2 \times pivot \times T_{ari} + T_{qadj}$

**Table 6.** Summary of the duration of the data exchange session in the EPC protocol.

Type of Time Slot	The Duration of the Time Slot
Identification	$T_1 + T_{PreTR} + 17 \times T_{pri} + T_2 + T_{FS} + T_{ACK} + T_1 + T_{PreTR} + 129 \times T_{pri} + T_2$
Empty slot	$T_1 + T_3$
Collision	$T_1 + T_{PreTR} + 17 \times T_{pri} + T_2$
Incorrect identification	$T_1 + T_{PreTR} + 17 \times T_{pri} + T_2 + T_{FS} + T_{ACK} + T_1 + T_3$

Multiple RFID systems use techniques based on TDMA methods. In the case of systems based on the EPC protocol, the multiple access protocol is based on the DFSA method. This method differs from FSA in that it allows dynamic adjustment of the number of slots in the data frame. The number of time slots in the frame, called the *Inventory Round*, is selected by the RWD on the basis of the *Q* parameter according to dependence:

$$T_{bTR} = \frac{M}{BLF} = M \times T_{pri} \tag{14}$$

where *Q* can vary from 2–15.

The inventory round is initiated by the *Query* command, in the syntax of which the *Q* parameter is sent to the transponders. On its basis, each transponder generates a random number in the range from 0 to  $2Q-1$ , called the *SC (Slot Counter)*, which is decremented by 1 after receiving the command *QueryRep*. The transponders that drew the number zero respond immediately after the *Query* command, while the remaining transponders whose *SC* number is greater than zero go into the arbitration state and wait for the next *QueryRep* commands or in the case of the need to correct the number of slots in the *QueryAdjust* inventory round. In the case of correct sending of its electronic product code EPC, the transponder goes into the *Invetoried* state. The RWD issues the *QueryRep* command, starting the next slot and changing the inventory flag of the previously recognized transponder, and waits for data from subsequent transponders. It should be emphasized that the time for which the recognition flag is held can be defined and is up to 5 s. The *QueryRep* command starts each subsequent slot in the inventory round. If more than one transponder answers the queries or none of the transponder’s answers, undesirable phenomena such as collisions and empty slots may occur in a given slot. Problems with the appearance of two or more

collisions or empty slots (none of the transponders are engaged in data exchange) are solved by the RWD by using the *QueryAdjust* commands.

Using this command, it is possible to increase or decrease the *Q* parameter. The inventory round is shortened or extended (Figure 8) and unrecognized transponders involved in the inventory round generate new values of the SC counter.

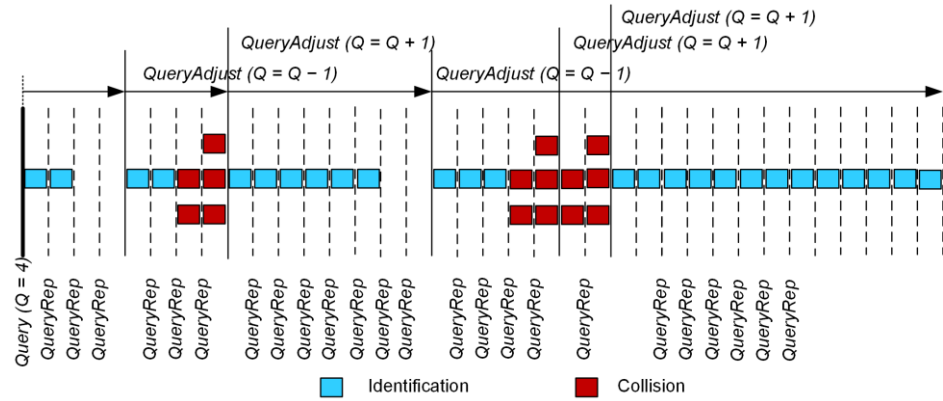


Figure 8. DFSA multiple access method in EPC protocol.

### 2.2. Conception of Laboratory IoTT Stand

In order to verify the prepared communication model, the laboratory stand was proposed (Figure 9). The effectiveness of object identification in the RFID system complied with the idea of IoTT can be tested in the stand.

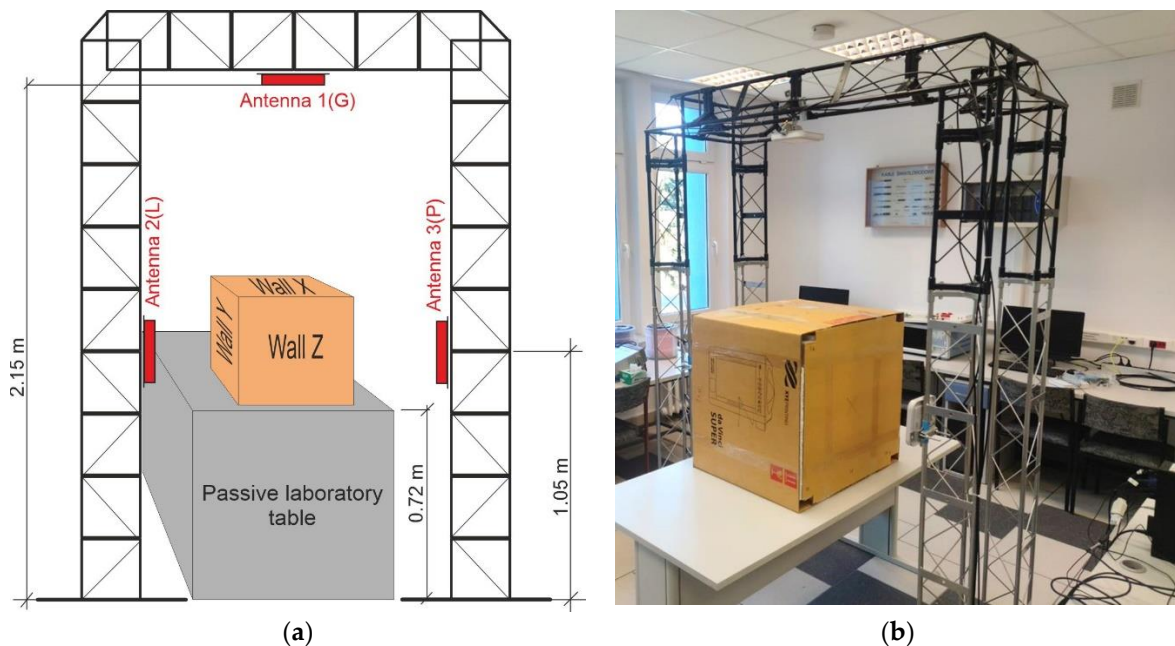
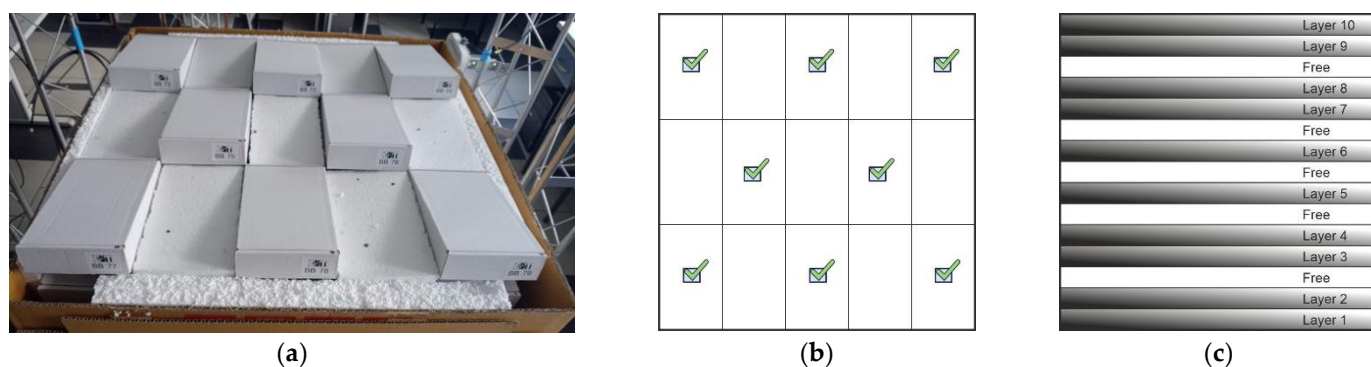


Figure 9. Laboratory stand to verify the basic assumptions of the communication model: (a) mutual location of RWD antennas and cube cardboard box walls X, Y, Z; (b) laboratory stand (localization of three RWD antenna around the cube carton).

In accordance with the considered concept of the IoTT logistics system, the communication model assumes the ability to read at least 50 fabric products labeled with the RFIDtex tags. The objects under identification are to be placed in a 60 cm cube carton (standard packaging of industry partner’s products), and the inventory time should not be longer than 10 s. The antenna of the RWD is to be placed at a distance of 1 m from the furthest product location. The communication protocol is to enable the recording and reading of

additional information, such as the EAN-13 code, season, purchase order, production batch, etc. using the number of bits not greater than it is possible in relation to the so-called user's internal memory of commercially available RFID chips.

In order to allow the verification of the communication model for the assumed IoTT system, the cardboard box with a side length of 70 cm is filled with objects as in Figure 10. The objects are intentionally in the form of small boxes with the RFIDtex tag on one side to arrange the operating space in a strictly defined way—the position of each transponder in the interrogation zone can be precisely indicated. The cardboard box is a bit larger than assumed cube space of IoTT. It facilitates the arrangement of the identified objects in the operating space of 60 cm cube, but the small boxes cannot move when the cardboard box is turned. The free space is filled with dielectric material (polystyrene) which dielectric permittivity is close to the air.



**Figure 10.** Implementation of design assumptions: (a) Cardboard box filled with small boxes with attached RFIDtex tags placed in a fixed and known location (Figure 1b); (b) Horizontal arrangement of objects; (c) Vertical arrangement of objects.

The applied layered methodology of even and unambiguous arrangement 80 objects on 15 layers (10 occupied and 5 free) allows authors to find the location of the product at any time and confirm the effectiveness of its identification. The transponders described with numbers from BB00 to BB79 are arranged sequentially starting from layer 1, and on each layer sequentially counting from the upper left corner (Figure 10b,c). The cardboard box and thus the location of each tag in relation to the RWD antennas, is clearly marked: wall X corresponds to the upper surface of the object (small box), opposite to the one labeled with RFIDtex tag, Y—to the side with a smaller surface, and Z—to the side with a larger surface. The arrangements of active RWD antennas used in experiments are also defined:

- 1AG—one upper antenna with number 1(G);
- 2AGL—two antennas, upper with number 1(G) and left side with number 2(L);
- 2ALR—two antennas, left side with number 2(L) and right side with number 3(R);
- 3AGLR—three antennas are active.

The cardboard is always positioned centrally relative to the plane of the RWD antennas and six variants are considered (Figure 9):

- W1 X1—wall X is set against the antenna 1(G), wall Z against 2(L) => 1X/2Z
- W2 X2—wall X is set against the antenna 1(G), wall Y against 2(L) => 1X/2Y
- W3 Y1—wall Y is set against the antenna 1(G), wall X against 2(L) => 1Y/2X
- W4 Y2—wall Y is set against the antenna 1(G), wall Z against 2(L) => 1Y/2Z
- W5 Z1—wall Z is set against the antenna 1(G), wall X against 2(L) => 1Z/2X
- W6 Z2—wall Z is set against the antenna 1(G), wall Y against 2(L) => 1Z/2Y.

### 3. Results

#### 3.1. Dependence of Identification Efficiency on the Number of Objects—Simulation Results

The identification efficiency was considered in the numerical model in which the number of transponders entering the interrogation zone was the main parameter. The range of variability of this parameter is set from 20 tags per second to 150 tags/s. Moreover, the research includes other parameters as:

- transmission coding technique: FM0 and Miller for  $M = 4$  and  $M = 8$ ;  $M$  means how many BLF frequency periods there are per bit of transmitted data;
- backscatter link frequency  $BLF$ : 40, 160 and 640 kHz;
- maximal duration of inventory round  $T_{max}$ : 0.1 s, 0.5 s and 1 s;
- persistence time of transponder: 1 s and infinity.

For different coding methods (FM0, Miller), there are clear differences in identification probabilities between FM0 and Miller technique (Figure 11a). In the case of using the FM0 coding, the initial increase in the identification probability is visible for its average values. It is due to the fact that in the case of identifying a small number of objects in one inventory round, the system "waits" until the maximum duration of the round is reached (set to 100 ms). This process is very short in the case of FM0 coding. It can be concluded that as long as the number of objects per round is not large, and consequently their identification time is equal to or less than the maximum duration of the inventory round, the probability to read moving objects will increase.

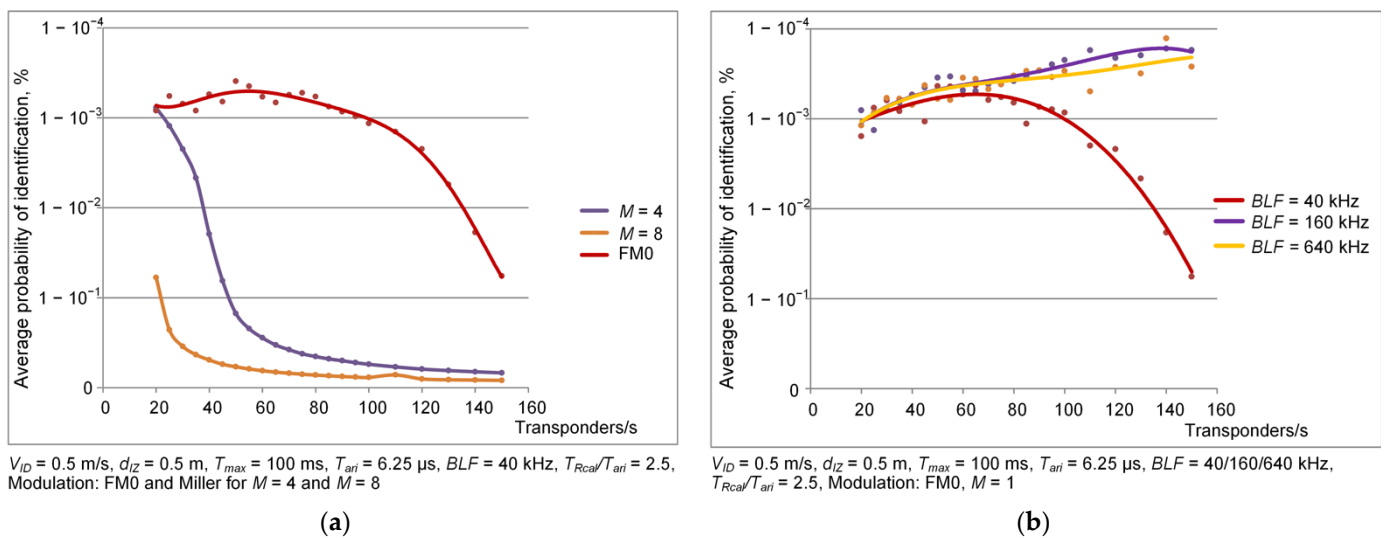


**Figure 11.** Average identification probability vs. the number of transponders in the IZ: (a) Different types of transmission coding; (b) Different  $BLF$  frequency;  $V_{ID}$ —speed of moving transponders,  $T_{ari}$ —reference timeframe,  $T_{Rcal}$ —calibration symbol of communication in transponder-RWD direction.

In the case of Miller coding, the probability to read transponders decreases much faster. This decrease is most noticeable when using the type of coding in which there are eight subcarrier periods per one symbol of the transmitted data ( $M = 8$ ). It significantly extends the duration of the inventory round, and then it is often interrupted due to the limitation of its duration. For more objects entering the IZ, the losses increase from round to round because of prematurely interrupting the inventory rounds. It results in a sudden drop in the identification probability.

In Figure 11b, the impact of  $BLF$  frequency changes is present. The  $BLF$  parameter determines the speed of data transmission between the transponders and the read/write device. A clear decrease in the probability of identification is visible at the value of 40 kHz. In the other two cases, an increase in the probability can be observed. This can be explained by the fact that as the  $BLF$  increases, the speed of data transmission between the tags and

the RWD also increases, and in consequently the duration of the transmitted symbols is shortened. For this reason, in a single inventory round with the assumed maximum duration, it is possible to identify more objects than in the case of the smallest value of the subcarrier frequency. At the 160 kHz frequency, a slight decrease in the probability of identification above 140 tags/s is visible, while at 640 kHz there is no any perturbations.

Interesting calculation results are obtained for two different values of the maximum duration of the inventory round (Figure 12a). The use of an inventory round with a longer duration does not guarantee an increase in the identification probability with a large number of moving objects. Nevertheless, the identification efficiency is satisfactory for the assumptions supposed in the both cases.

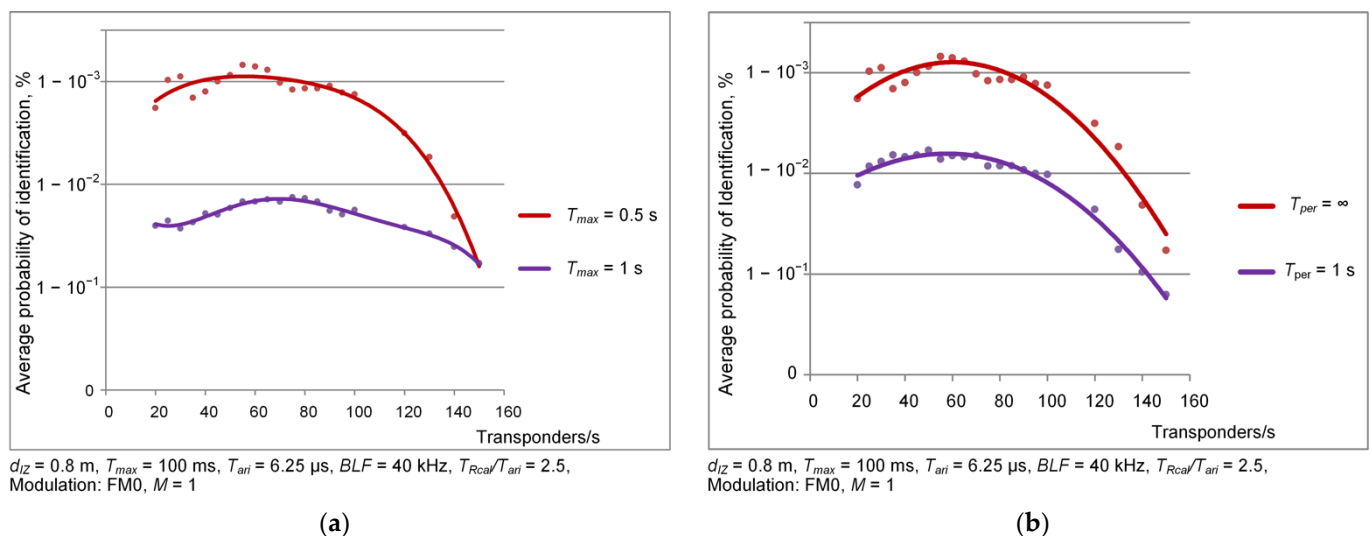


**Figure 12.** Average identification probability vs. number of transponders in IZ: (a) Different maximal duration of inventory round; (b) Different persistence time.

The visible (Figure 12a) decrease in the identification probability value in the case of setting a longer inventory round results from the fewer number of attempts to read the transponders when they move through the IZ. In the case of shorter rounds, subsequent objects entering the interrogation zone are read more often, even if they are not recognized in one of the first rounds, there is a greater chance of correct identification in the next once.

Readers should also pay their attention to the comparison of the identification probability in the ideal case, when the persistence time is infinite, and the transponders are read only once, with the real case, in which this parameter has a finite value (Figure 12b). When the objects are identified several times ( $T_{per} = 1$  s) the identification probability is bigger.

The obtained results of analyzes and simulations indicate that the specified assumptions regarding the number of identified objects and the size of the interrogation zone are possible to implement in practice. The user has a great deal of freedom in choosing the parameters of the communication protocol. Nevertheless, the use of the Miller code on the transponder-RWD link should be avoided, as it does not guarantee the assumed effectiveness of identification.

Simulations of the effectiveness of identification as a function of the size of the interrogation zone and the speed of transponders movement in this area are presented in Figure 13.

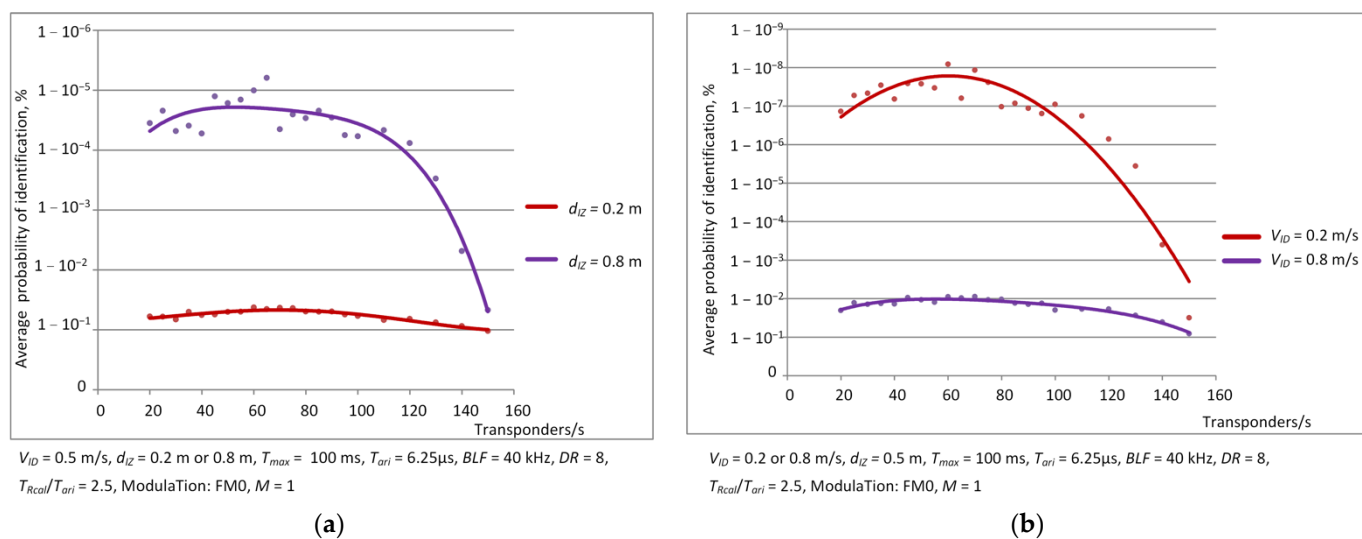


**Figure 13.** Dependence of average probability of identification vs. number of transponders included in IZ at: (a) Different IZ sizes; (b) Different speeds of arriving transponders.

In the case of simulations carried out for different IZ size values (Figure 13a), the difference between the identification probability value for the zone of 0.2 m and 0.8 m is clearly visible. Some increase in its value with the increase in the number of transponders can also be explained by the fact that the number of identifications in single inventory rounds is gradually increasing. However, when the transponders leave the system IZ, the large number of transponders lost causes that the probability of identification in the case of using a small zone size remains at a low level. Using an  $d_{IZ}$  of 0.8 m gives much better results. The probability of identification remains high, and its clear decrease is visible only if the number of transponders exceeds 120 id/s. It is similar in the case of the results obtained for two different tag velocities arriving in the area (Figure 13b). Of course, the probability of identification is higher if the transponders move slower (0.2 m/s), but it is definitely lower if the tags move faster through the IZ (0.8 m/s). The initial increase in read probability is due to similar reasons as in the previous simulations.

The obtained results of analyzes and simulations indicate that the assumptions as to the number of transponders and the size of the IZ, specified at the designing stage of project and adopted for implementation, are feasible in practice. The obtained results, of course, require practical verification, which will be carried out as part of further work at the next stages of the project.

### 3.2. Dependence of Identification Efficiency on the Number of Objects—Measurement Results

The dynamic anti-collision RFID system, in which the use of RFIDtex transponders is assumed, were simulated in the numerical calculations. On the base of developed model, the best combination of communication protocol parameters, from the point of view of identification efficiency, were obtained. It was stated, among others, that the Miller code should not be used, the optimal number of RFIDtex transponder equals 80 items for assumed environment of IoT, etc. All conclusions drawn from the simulations were applied in the experimental stage.

In accordance with the assumptions of the developed numerical model, the identification effectiveness in the prepared cardboard box filled with RFIDtex products was tested in laboratory measurements. In prepared configurations of test experiments, series of 100 measurements were made for every setting. The identification efficiency was measured using a single RWD with a multiplexer supporting one, two or three active antennas arranged as in Figure 9a. Tests were made for three settings of transponders according to the plane determined by the radiator of RWD antenna No. 1 (G): (1) parallel to the plane, (2) perpendicular to the plane and (3) perpendicular but rotated by  $90^\circ$  to the

plane. The measurements were carried out for the RWD output power equals 1 W and 2 W EIRP (Effective Isotropic Radiated Power). In all tests only FM0 coding was used on the transponder-RWD link.

The identification effectiveness for six predefined settings of objects in relation to the RWD antennas is presented in Figure 14. The case of parallel placement of transponders relative to antenna No. 1 (G) is summed in Figure 14a. The bars were obtained for a single antenna (1AG) as well as more antennas (e.g., 2AGL, 3AGRL—see Section 2.2), for two previously defined values of RWD output power. It is clearly visible that in the case of a single antenna, the identification efficiency is the lowest, although it is consistent with the numerical model. Increasing the number of antennas allows the authors to achieve almost 100% readability. Certainly, such results are related to the improved transponder power supply conditions, but also to the increased number of correctly conducted inventory rounds. Because in the target environment of IoTT system, the identified objects may be oriented in relation to the antenna in different ways, the test also were performed for transponders rotated by 180° (Figure 14b). As in the case W1, a high 100% identification efficiency is achieved.

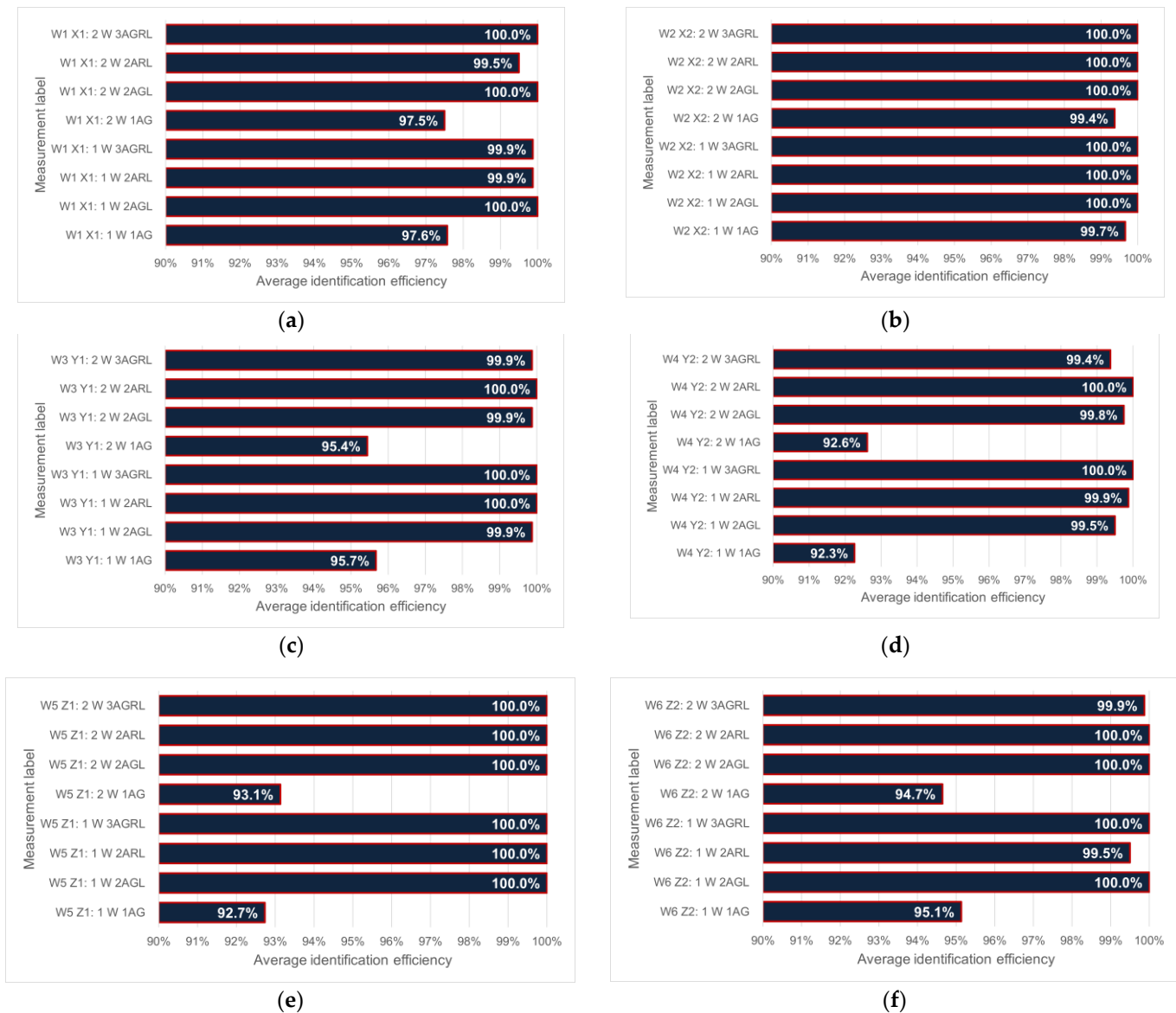


**Figure 14.** Comparison of average identification efficiency for settings: (a) W1; (b) W2; (c) W3; (d) W4; (e) W5; (f) W6; detailed explanation of descriptions for test setups is included in Section 2.2.

Results of measurements in the case of perpendicular positioning of the transponders in relation to the antenna No. 1 (G) are summed up in Figure 14c,d. It should be noticed that when the transponders are turned by  $180^\circ$  (Figure 14d), a significant decrease in the identification efficiency is visible for one RWD antenna. This is related to the operating conditions of the transponders—they have to operate with mismatched polarization of the tag antennas and the RWD antenna. The situation is at once improved by using more antennas.

A summary of the measurement results in the case of the perpendicular arrangement of the transponders in relation to the planes of the antennas is shown in Figure 14e,f. As previously, the tests are also conducted for tags rotated by  $180^\circ$  (Figure 14f). A further decrease in the identification effectiveness for the system with only one antenna is visible. This is related to the operating conditions of the transponders, which have to work in a system with mismatched polarization of the antenna systems. The situation is improved by using the multiplexer with more active RWD antennas. In this case, the identification efficiency is at a satisfactory level.

Figure 15 presents the measurements of the average identification efficiency for all positions of objects in space of the IZ. When only one RWD antenna is used (Figure 15a), the identification efficiency strongly depends on the orientation of objects in space. The efficiency decreases when the transponder antennas are placed perpendicular to the plane of the RWD antenna. However, a high identification efficiency, consistent with the numerical model, is observed in each case of the assumed parameters of IoTT system.

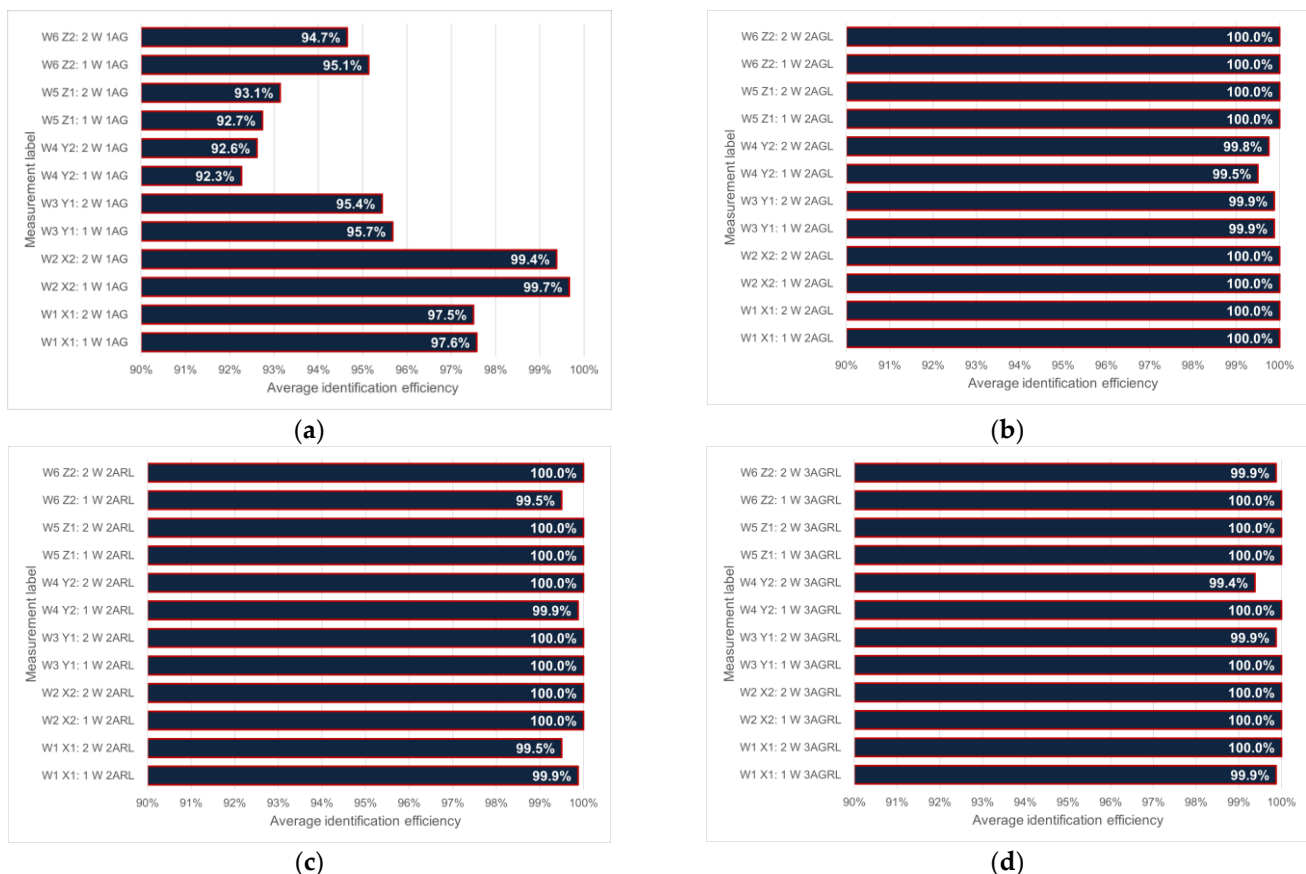


**Figure 15.** Comparison of average identification efficiency for active antennas: (a) 1AG; (b) 2AGL; (c) 2ARL; (d) 3AGRL; detailed explanation of descriptions for test setups is included in Section 2.2.

With three RWD antennas (Figure 15d) it is possible to reach 100% identification efficiency in all arrangements. The achieved results prove that it is possible to obtain the identification efficiency at the level of 100%. Nevertheless, it should be noted that the

95% efficiency is not bad and can still be improved by repeating scans and appropriate post-processing of the results.

The last test was for different values of the RWD output power of 1 W (Figure 16a) and 2 W EIRP (Figure 16b), for all spatial configurations of the cardboard positions and RWD antennas. The results show a clear dependence of the identification efficiency on the number of active RWD antennas. As mentioned earlier, this is related to the improvement of the conditions for supplying the transponders and the increase in the number of inventory rounds repeated with success.

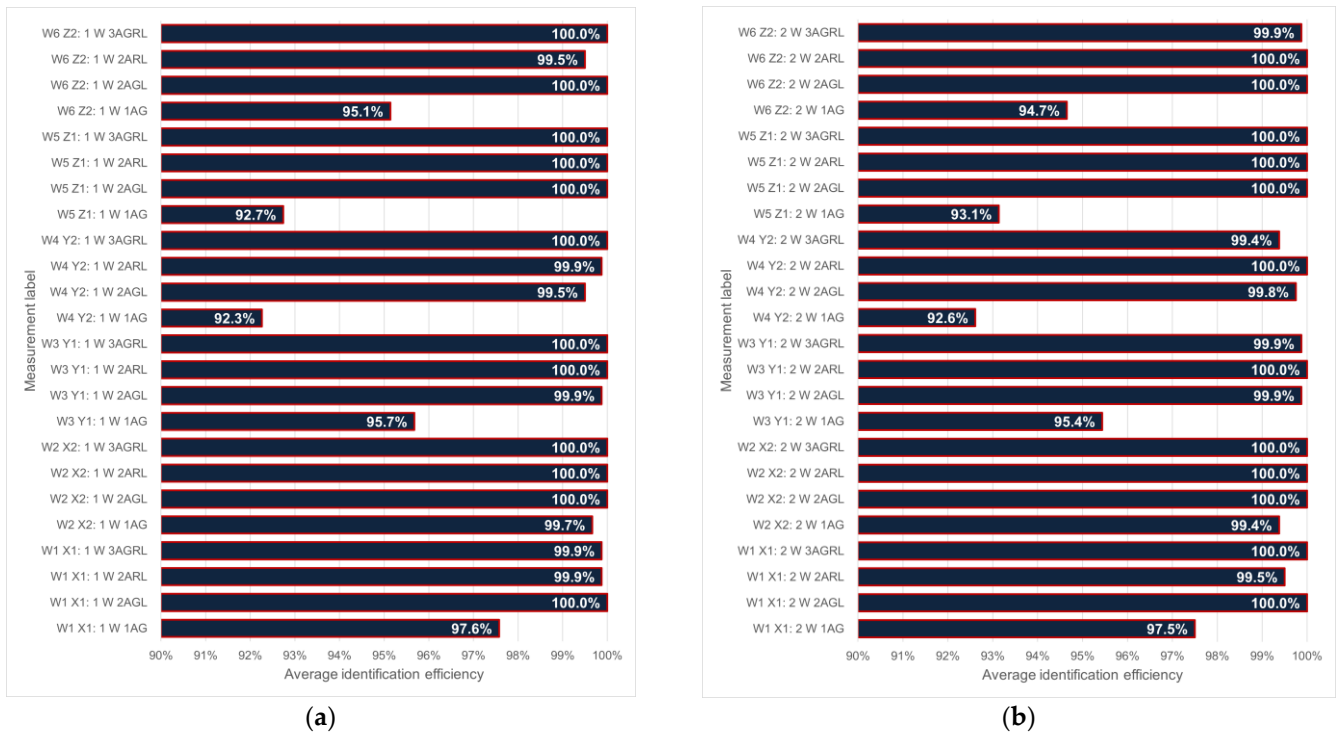


**Figure 16.** Comparison of average identification efficiency for output power: (a) 1 W; (b) 2 W; Detailed explanation of descriptions for test setups is included in Section 2.2.

The main conclusion carried out from the simulations and measurements is that the system is capable of effectively identifying a group of objects expected to be transported in a cardboard box. The most important parameter ensuring effective data reading is the number of antennas connected to the RWD. For the expected number of objects, the parameters of the communication protocol (apart from the transmission code on the transponders-read/write device link) do not affect the reduction of identification efficiency.

#### 4. Conclusions

The performed analyzes and simulations were subjected to practical verification on a specially prepared laboratory stand. The identification efficiency was measured using a single read/write device with one, two or three antennas and output power equals 1 W or 2 W EIRP. Additionally, the experiment was made for different orientations and localizations of the transponders' antennas in relation to the RWD antennas. The obtained results prove that within the scope of the assumed number of RFIDtex transponders, the user has a great freedom in choosing the parameters of the communication protocol. Moreover, the most important parameter that ensures effective data reading is the number of antennas connected to the read/write devices. During identification processes, the use of the Miller code on the transponders-RWD link should be avoided, as it does not guarantee the assumed effectiveness.

The simulations also show that the highest efficiency of identification for various sets of protocol parameters is obtained in the range of 60–80 transponders registered per second. For this volume of objects, the respective parameters can be selected in the widest range. For higher number of tags the identification can be also performed with the assumed efficiency but some of the parameters have to be restricted to specific values. A good example of such a case is the BLF frequency and the transmission coding used—any change of each may have a significant impact on increasing or decreasing the identification efficiency. Another pair of parameters is the maximum duration of the inventory round or the persistence time that determine the efficiency in the entire simulated range of the number of tags.

Based on the results obtain form the numerical model, it was decided to select a representative group of products/objects/transponders at the level of 80 pcs. The validity of the proposed approach to the experiment was confirmed on the basis of performed verification by multiple readings of the efficiency parameter for different spatial allocations of transponders, different ways of locating RWD antennas, and different output powers set in read/write devices. The achieved level of identification efficiency corresponds to the assumptions and results obtained from the simulation and it definitively meets the conditions of RFIDtex practical implementation.

**Author Contributions:** Conceptualization, B.P. and G.L.; methodology, B.P. and K.K.; software, B.P.; validation, P.J.-M. and M.W.; formal analysis, K.K. and M.S.; investigation, K.K. and M.S.; resources, K.K. and M.S.; data curation, B.P.; writing—original draft, M.W.; writing—review & editing, M.W.; visualization, B.P. and M.W.; supervision, B.P.; project administration, P.J.-M.; funding acquisition, P.J.-M. and M.W. All authors have read and agreed to the published version of the manuscript.

**Funding:** This research paper was developed under the project financed by the Minister of Education and Science of the Republic of Poland within the “Regional Initiative of Excellence” program for years 2019–2023. Project number 027/RID/2018/19, amount granted 11 999 900 PLN. The laboratory stand built under the program „EMC-LabNet—Polish Network of EMC Laboratories” (no POIR.04.02.00-02-A007/16) was used in the research experiments. Program funding source: Smart Growth Operational Programme 2014–2020; Priority Axis IV: Increasing the Research Potential; Measure 4.2: Development of Modern Research Infrastructure of the Science Sector.

**Institutional Review Board Statement:** Not applicable.

**Informed Consent Statement:** Not applicable.

**Data Availability Statement:** All calculated and measured data will be provided upon request to the correspondent authors by email with appropriate justification.

**Conflicts of Interest:** The authors declare no conflict of interest. The funders had no role in the design of the study; in the collection, analyses, or interpretation of data; in the writing of the manuscript; or in the decision to publish the results.

## References

1. Finkenzeller, K. *RFID Handbook—Fundamentals and Applications in Contactless Smart Cards, Radio Frequency Identification and Near-Field Communication*, 3rd ed.; Wiley: Hoboken, NJ, USA, 2010.
2. Dobkin, D.M. *The RF in RFID: UHF RFID in Practice*, 2nd ed.; Newnes: Oxford, UK, 2012.
3. Honarvar, M.G.; Latifi, M. Overview of wearable electronics and smart textiles. *J. Text. Inst.* **2017**, *108*, 631–652. [[CrossRef](#)]
4. Koncar, V. *Introduction to Smart Textiles and Their Applications*; Elsevier: Amsterdam, The Netherlands, 2016; ISBN 9780081005835.
5. Schneegas, S. *Smart Textiles Fundamentals, Design, and Interaction*; Springer: New York, NY, USA, 2017; ISBN 978-3-319-50123-9.
6. Moraru, A.; Helerea, E.; Ursachi, C.; Călin, M.D. RFID system with passive RFID tags for textiles. In Proceedings of the 10th International Symposium on Advanced Topics in Electrical Engineering (ATEE), Bucharest, Romania, 23–25 March 2017.
7. Virkki, J.; Wei, Z.; Liu, A.; Ukkonen, L.; Björninen, T. Wearable passive E-textile UHF RFID tag based on a slotted patch antenna with sewn ground and microchip interconnections. *Int. J. Antennas Propag.* **2017**, *2017*, 3476017. [[CrossRef](#)]
8. Moraru, A.; Ursachi, C.; Helerea, E. A New Washable UHF RFID Tag: Design, Fabrication, and Assessment. *Sensors* **2020**, *20*, 3451. [[CrossRef](#)]
9. Ukkonen, L.; Sydänheimo, L.; Rahmat-Samii, Y. Sewed textile RFID tag and sensor antennas for on-body use. In Proceedings of the 6th European Conference on Antennas and Propagation, Prague, Czech Republic, 25–30 March 2012.
10. Luo, C.; Gil, I.; Fernández-García, R. Wearable Textile UHF-RFID Sensors: A Systematic Review. *Materials* **2020**, *13*, 3292. [[CrossRef](#)] [[PubMed](#)]

11. Corchia, L.; Monti, G.; Tarricone, L. Wearable antennas: Nontextile versus fully textile solutions. *IEEE Antennas Propag. Mag.* **2019**, *61*, 71–83. [[CrossRef](#)]
12. Lai, Y.-C.; Chen, S.-Y.; Hailemariam, Z.L.; Lin, C.-C. A Bit-Tracking Knowledge-Based Query Tree for RFID Tag Identification in IoT Systems. *Sensors* **2022**, *22*, 3323. [[CrossRef](#)]
13. Arjona, L.; Landaluce, H.; Perallos, A.; Onieva, E. Dynamic Frame Update Policy for UHF RFID Sensor Tag Collisions. *Sensors* **2020**, *20*, 2696. [[CrossRef](#)]
14. Filho, I.E.D.B.; Silva, I.; Viegas, C.M.D. An Effective Extension of Anti-Collision Protocol for RFID in the Industrial Internet of Things (IIoT). *Sensors* **2018**, *18*, 4426. [[CrossRef](#)]
15. Huang, Z.; Xu, R.; Chu, C.; Li, Z.; Qiu, Y.; Li, J.; Ma, Y.; Wen, G. A Novel Cross Layer Anti-Collision Algorithm for Slotted ALOHA-Based UHF RFID Systems. *IEEE Access* **2019**, *7*, 36207–36217. [[CrossRef](#)]
16. Fu, Z.; Deng, F.; Wu, X. Design of a Quaternary Query Tree ALOHA Protocol Based on Optimal Tag Estimation Method. *Information* **2017**, *8*, 5. [[CrossRef](#)]
17. Lin, Y.-H.; Liang, C.-K. A Highly Efficient Predetection-Based Anticollision Mechanism for Radio-Frequency Identification. *J. Sens. Actuator Netw.* **2018**, *7*, 13. [[CrossRef](#)]
18. Vales-Alonso, J.; Bueno-Delgado, V.; Egea-Lopez, E.; Gonzalez-Castano, F.J.; Alcaraz, J. Multiframe Maximum-Likelihood Tag Estimation for RFID Anticollision Protocols. *IEEE Trans. Ind. Inform.* **2011**, *7*, 487–496. [[CrossRef](#)]
19. Alcaraz, J.J.; Vales-Alonso, J.; Egea-Lopez, E.; Garcia-Haro, J.J. A Stochastic Shortest Path Model to Minimize the Reading Time in DFSA-Based RFID Systems. *IEEE Commun. Lett.* **2013**, *17*, 341–344. [[CrossRef](#)]
20. Arjona, L.; Landaluce, H.; Perallos, A.; Onieva, E. Timing-Aware RFID Anti-Collision Protocol to Increase the Tag Identification Rate. *IEEE Access* **2018**, *6*, 33529–33541. [[CrossRef](#)]
21. Guo, K.; Xie, X.; Qi, H.; Li, K. A High Time-Efficient Missing Tag Detection Scheme for Integrated RFID Systems. *Sensors* **2022**, *22*, 4601. [[CrossRef](#)]
22. Espin, J.J.A.; Egea-Lopez, E.; Vales-Alonso, J.; Haro, J.G. Dynamic system model for optimal configuration of mobile RFID systems. *Comput. Netw.* **2011**, *55*, 74–83.
23. Pawłowicz, B.; Trybus, B.; Salach, M.; Jankowski-Miśkiewicz, P. Dynamic RFID Identification in Urban Traffic Management Systems. *Sensors* **2020**, *20*, 4225. [[CrossRef](#)]
24. Standard International Organization for Standardization/International Electrotechnical Commission. *Information Technology—Radio Frequency Identification for Item Management—Part 63: Parameters for Air Interface Communications at 860 MHz to 960 MHz Type C*; ISO/IEC: Geneva, Switzerland, 2015; p. 18000-63.
25. Sabat, W.; Klepacki, D.; Kamuda, K.; Kuryło, K. Analysis of Electromagnetic Field Distribution Generated in a Semi-Anechoic Chamber in Aspect of RF Harvesters Testing. *IEEE Access* **2021**, *9*, 92043–92052. [[CrossRef](#)]
26. NXP: SL3S1214 UCODE 7m. Available online: [www.nxp.com](http://www.nxp.com) (accessed on 11 April 2022).
27. GS1 EPCglobal. *EPC Radio-Frequency Identity Protocols Generation-2 UHF RFID; Specification for RFID Air Interface Protocol for Communications at 860 MHz–960 MHz, Ver. 2.1*; EPCglobal: Brussels, Belgium, 2018.
28. Jankowski-Miśkiewicz, P.; Węglarski, M.; Chamera, M.; Pyt, P. Textronic UHF RFID Transponder. *Sensors* **2021**, *21*, 1093. [[CrossRef](#)]
29. Pei, J.; Fan, J.; Zheng, R. Protecting Wearable UHF RFID Tags with Electro-Textile Antennas: The Challenge of Machine Washability. *IEEE Antennas Propag. Mag.* **2021**, *63*, 43–50. [[CrossRef](#)]
30. Węglarski, M.; Jankowski-Miśkiewicz, P. Factors Affecting the Synthesis of Autonomous Sensors with RFID Interface. *Sensors* **2019**, *19*, 4392. [[CrossRef](#)] [[PubMed](#)]
31. Gupta, A.; Asad, A.; Meena, L.; Anand, R. IoT and RFID-based Smart Card System Integrated with Health Care, Electricity, QR and Banking Sectors. In *Artificial Intelligence on Medical Data, Proceedings of International Symposium, ISCMM 2021, Sikkim, India, 11–12, November 2021*; Gupta, M., Ghatak, S., Gupta, A., Mukherjee, A.L., Eds.; Springer Nature: Singapore, 2022.
32. Gupta, A.; Srivastava, A.; Anand, R.; Chawla, P. Smart Vehicle Parking Monitoring System Using RFID. *Int. J. Innov. Technol. Explor. Eng.* **2019**, *8*, 225–229.

**Disclaimer/Publisher’s Note:** The statements, opinions and data contained in all publications are solely those of the individual author(s) and contributor(s) and not of MDPI and/or the editor(s). MDPI and/or the editor(s) disclaim responsibility for any injury to people or property resulting from any ideas, methods, instructions or products referred to in the content.